Received: 13 March 2019 | Revised: 18 July 2019 | Accepted: 19 July 2019

DOI: 10.1002/dep2.80

SPECIAL ISSUE ARTICLE

The Depositional Record Open Access
A journal of the International Association of Sedimentologists
WILEY

Lateral facies variations in the Triassic Dachstein platform: A challenge for cyclostratigraphy

Elias Samankassou[1] | **Paul Enos**[2]

[1]Department of Earth Sciences, University of Geneva, Geneva, Switzerland

[2]Department of Geology, University of Kansas, Lawrence, KS, USA

Correspondence
Elias Samankassou, Department of Earth Sciences, University of Geneva, Geneva, Switzerland.
Email: elias.samankassou@unige.ch

Funding information
van Sant Fund and Haas Fund, University of Kansas; Schweizerischer Nationalfonds zur Förderung der Wissenschaftlichen Forschung; Deutsche Forschungsgemeinschaft, Grant/Award Number: FL 42/81

Abstract

The Triassic Dachstein platform limestone at Steinernes Meer, Salzburg, Austria, includes 611 m of limestone with 222 peritidal cycles overlain by 273 m of subtidal, non-cyclic and weakly cyclic limestone. Cycle patterns include both shoaling and deepening upward, symmetrical, truncated, and couplets without a depth vector. Beds are laterally discontinuous, and cycle bounding surfaces are laterally variable in the studied strata. Of 558 subtidal and intertidal beds measured, 121 (21.7%) disappear laterally. An additional 73 beds (13.1%) show significant (>10%) lateral variations in thickness. Mean thickness variation is 49%. Both lateral variations and terminations appear to lack a spatial vector. Disappearances toward the inferred platform interior (west) total 10% of the beds. East, toward the platform margin, 11.6% of the beds disappear. Thickness changes occur in 6.5% of beds in each direction. The lack of lateral continuity of beds precludes a simple allocyclic forcing model and is consistent with a non-eustatic component to stratification. Erosion of intertidal intervals is the process that can be most readily documented. Non-uniform rates of production, transport and distribution of sediments, superposed on stratigraphic sequences driven by eustasy, probably also contributed to the complex cycle patterns recorded in the Dachstein. Such composites of autocyclic and extrabasinal factors should not be uncritically interpreted as exclusive records of orbital forcing. Lateral discontinuities and thickness variations would also produce inaccuracies in spectral analysis of thickness patterns, typically conducted in search of 'Milankovich frequencies', as well as in construction of Fischer plots to analyse long-period oscillations in accommodation. Any section subjected to cycle analysis should be examined for lateral changes, to the extent permitted by the exposures, in order to produce the most complete (composite) section possible.

KEYWORDS

Austria, autocyclic processes, carbonate-platform cycles, lateral variations, Northern Calcareous Alps, Triassic

1 | INTRODUCTION

Shallow-water platform carbonates of all ages commonly show repetitive, cyclic patterns. Mechanisms proposed for cycle generation include (a) intrinsic or autocyclic processes and (b) externally imposed or allocyclic processes (Beerbower, 1964), namely eustatic sea-level changes and tectonic pulses (cf. Benedictis, Bosence, & Waltham, 2007; Bosence et al., 2009; Cisne, 1986; Fischer, 1964; Goldhammer, Dunn, & Hardie, 1987). Discussion has focused mainly on eustasy versus autocyclicity, specifically, lateral sediment progradation and redistribution (cf. Ginsburg, 1971; Lehrmann & Goldhammer, 1999). The Dachstein Limestone of the Northern Calcareous Alps may be considered the birthplace of cyclostratigraphy through the seminal work of Sander (1936), although he discussed 'rhythms' and never used the current term, 'cycle'. His student, Schwarzacher (1948, 1954), recognized five cycles in a megacycle and postulated orbital control. Fischer (1964) masterfully elucidated the sedimentary processes forming the Dachstein cycles and also speculated about orbital control on cycle development, in particular the obliquity cycle of approximately 41 kyr.

Cycle period is generally deduced by dividing the number of cycles in linearly measured sections into the elapsed time interval (typically poorly constrained for platform deposits). This assumes equal duration for all cycles and that all cycles are sampled within the section. Thus Fischer (1964, p. 144) estimated a duration of 50 kyr for a Dachstein cycle, but reasoned that the orbital periods of 20, 40 or 100 kyr were more likely.

Many workers have described laterally persistent platform cycles (Demicco, 1985; Goldhammer et al., 1987; Goldhammer, Dunn, & Hardie, 1990; Goodwin & Anderson, 1985; Grotzinger, 1986; Koerschner & Read, 1989; Osleger & Read, 1991), although lithofacies within individual cycles can vary laterally (Adams & Grotzinger, 1996; Bádenas, Aurell, & Bosence, 2010; Cloyd, Demicco, & Spencer, 1990; Cowan & James, 1996; Egenhoff, Peterhänsel, Bechstädt, Zühlke, & Grötsch, 1999; Laporte, 1967; Obermaier, Ritzmann, & Aigner, 2015; Pratt & James, 1986; Samankassou, Strasser, Di Gioia, Rauber, & Dupraz, 2003). Lateral facies variations have also been reported from modern sites (Bosence, 2008; Eberli, 2013; Enos & Perkins, 1979; Harris, Purkis, & Ellis, 2011; Purkis & Harris, 2016; Wilkinson & Drummond, 2004) and from the Triassic Dachstein platform in the Northern Calcareous Alps (Enos & Samankassou, 2002; Piller, 1976, 1981; Satterley, 1996b; Zankl, 1967).

The lateral facies variations that alter cycle numbers, thickness and character within the Dachstein Limestone at Steinernes Meer and Loferer Steinberge, Austria, are quantified here. This study emphasizes the importance of quantifying lateral persistence in the analysis of sedimentary cycles and provides quantitative data for carbonate depositional models (cf. Burgess, 2016; Burgess & Wright, 2003;

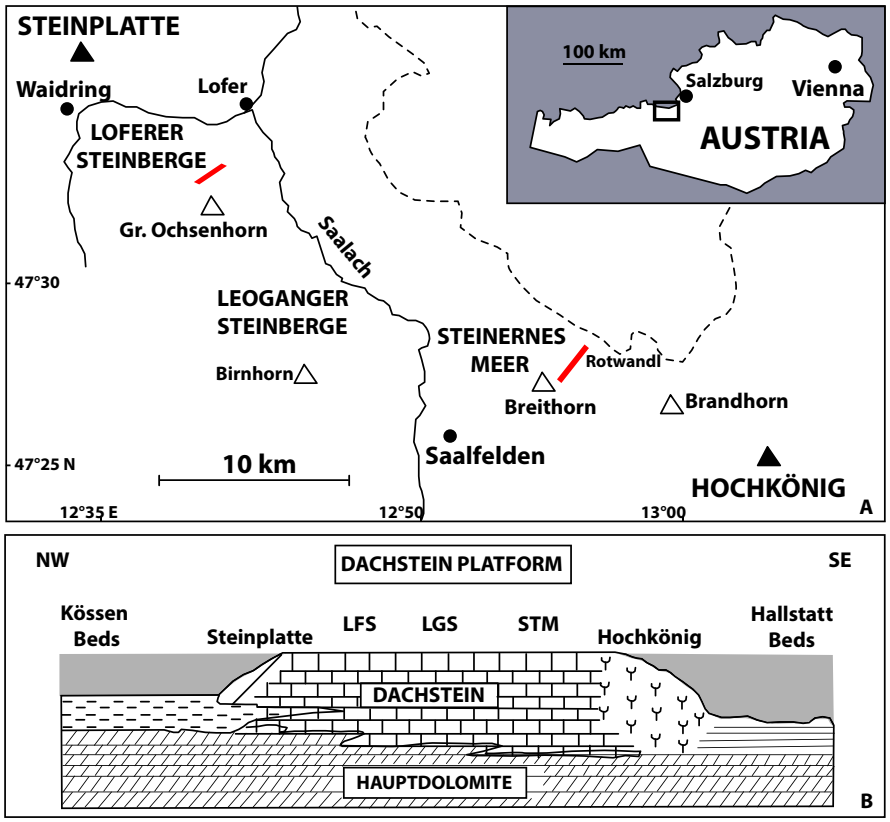

FIGURE 1 (A) Location of the measured sections in Steinernes Meer and Loferer Steinberge (respective bars) southwest of Salzburg, Austria. (B) Stratigraphic sketch of the Dachstein platform and the adjacent basins. LFS, Loferer Steinberge; LGS, Leoganger Steinberge; STM: Steinernes Meer

Burgess, Wright, & Emery, 2001; Le Blévec, Dubrule, John, & Hampson, 2018).

2 | LOCATION

The Dachstein platform is a large Late Triassic (Norian-Rhaetian) platform, which extends from the Steinplatte, bordered by the Kössen basin in the north-west, to the Hochköning reef and Hallstatt basin in the south-east (Figure 1A and B). Other Dachstein platforms are recognized across Austria (Krystyn, Mandl, & Schauer, 1991), Hungary (Haas, 1994), Slovenia (Celarc, Gale, & Kolar-Jurkovšek, 2014) and northern Italy, in the correlative Dolomia Principale (Hauptdolomit; Bosellini, 1967). The lower part of the Steinernes Meer section (0–631.5 m) extends from near the transition to the underlying Hauptdolomit below Breithorn (Figure 2A; 47°27.365′N, 12°54.480′E) to trail 428 at ~47°27.58′N, 12°54.63′E. The upper part (608–893.6 m) from 47°28.004′N, ~12°55.160′E, extending to the contact with the Jurassic Knollenkalk at Rotwandl (47°28.497′N, 12°55.384′E). The Loferer Steinberge section is located along the trail from the Schmidt-Zabierow Hutte to Grosser Reifhorn. The base is at the foot of the Wehrgube (47°32.991′N, 12°38.886′E), the top at approximately 47°32.57′N, 12°38.76′E.

3 | METHODS

An 894 m thick section measured at Steinernes Meer comprises most of the Dachstein interval, including the upper contact, at a scale of 40:1 (2.5 cm = 1 m). The section extends from near the transition to the underlying

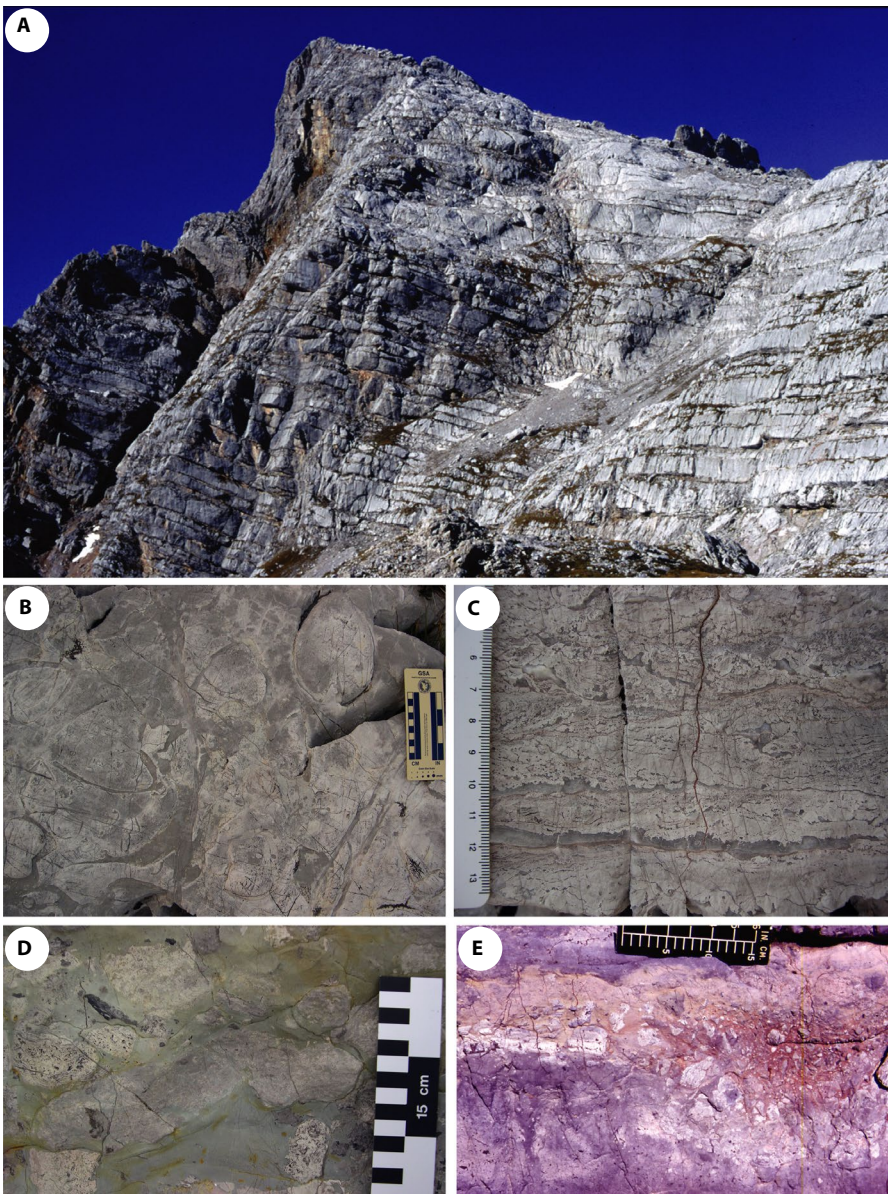

FIGURE 2 (A) Cyclic Dachstein Limestone below Breithorn at the south edge of Steinernes Meer. The lower 631 m of the Steinernes Meer section were measured here, as were the sections of Fischer (1964, his figs. 4 and 5B), Goldhammer et al. (1990, fig. 16), and the base of Satterley's (1996b, fig. 4). See also Enos and Samankassou (1998, fig. 4). (B) Megalodont lime packstone; member C. Cement-filled megalodont mould at upper left of scale and elsewhere in image. Steinernes Meer section. (C) Dolomitic mudstone with vague wavy lamination, aligned fenestrae, sheet cracks and some auto-brecciation; typical member B. Steinernes Meer section. Scale in centimetres. (D) Soilstone with rounded clasts of lime wackestone and fenestral dolomudstone in lime mudstone matrix; member A. (E) Red soilstone (member A) dominated by angular clasts of whitish dolomudstone with aligned fenestrae overlying and filling karstic depression within subtidal lime wackestone (member C). Steinernes Meer section, 411.3 m

Hauptdolomit to the contact with the Jurassic Knollenkalk. Cycles are well-developed in the basal 611 m, totalling 222 cycles. The interval from 611 to 810 m is essentially non-cyclic; only 11 cycles were logged within the 199 m of strata. The top 74 m of the Dachstein (810–884) is weakly cyclic, including 24 cycles. A 272 m section in the Loferer Steinberge, 22 km to the west, was measured at a scale of 80:1. It includes no formational contacts, but contains 93 peritidal cycles. The field logs record bedding features, Dunham textures, sedimentary and diagenetic structures, principle fossils, sedimentary particles, colour, and locations of photographs and samples. Subsequently each interval was classified according to Fischer's ABC 'members' (Figure 3, Fischer, 1964). This simplification is useful in the present context; for more detailed description and interpretation of facies, see Fischer (1964) and Enos and Samankassou (1998). The lateral continuity of beds was noted to the degree permitted by the outcrop (Figure 4), generally a few tens or hundreds of metres, by direct tracing; exceptionally up to 1.7 km by correlation.

4 | DATA

Most of the Dachstein is light-grey, structureless, lime packstone or wackestone with a moderately diverse biota, dominated by megalodont bivalves (Figure 2B; Enos & Samankassou, 1998). This is the megalodont limestone or subtidal 'member C' of Fischer (1964). Locally, ooids and thickets of arborescent corals are present, primarily in non-cyclic subtidal deposits. Member C comprises 56% of the beds and 92% of the total measured thickness (Table 1). Whitish dolomudstone exhibiting fenestrae, irregular millimetre lamination and/or desiccation cracks (Figure 2B) is 'member B' or 'loferite' of Fischer (1964), interpreted as intertidal and supratidal. It constitutes 31% of the beds but only

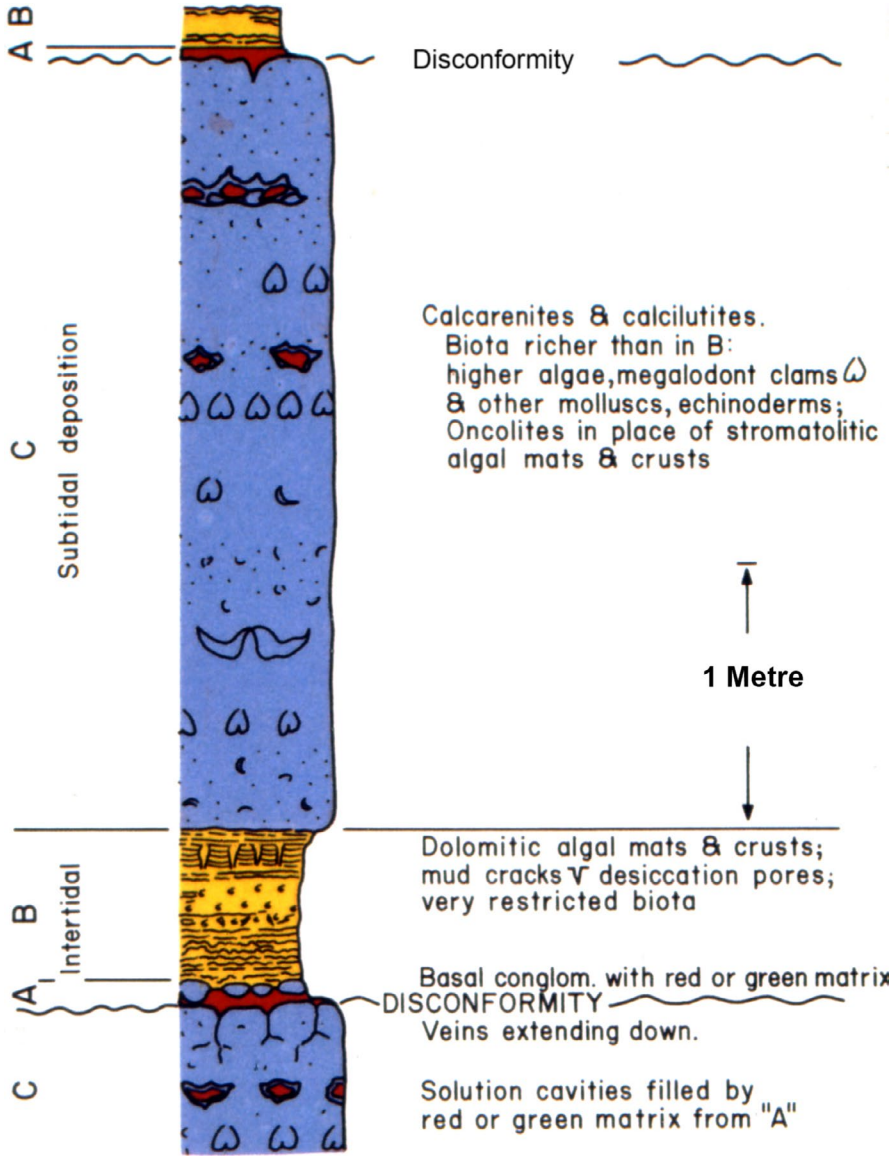

FIGURE 3 Fischer's 'Lofer cyclothem' (modified slightly from Fischer, 1964, p. 113). His member designations, A, B and C are used herein for the principle lithologies, as well as 'd' for disconformity. For more detailed lithologic descriptions, see Fischer (1964) and Enos and Samankassou (1998). Note that Fischer's cycle ABC(d) is deepening upward

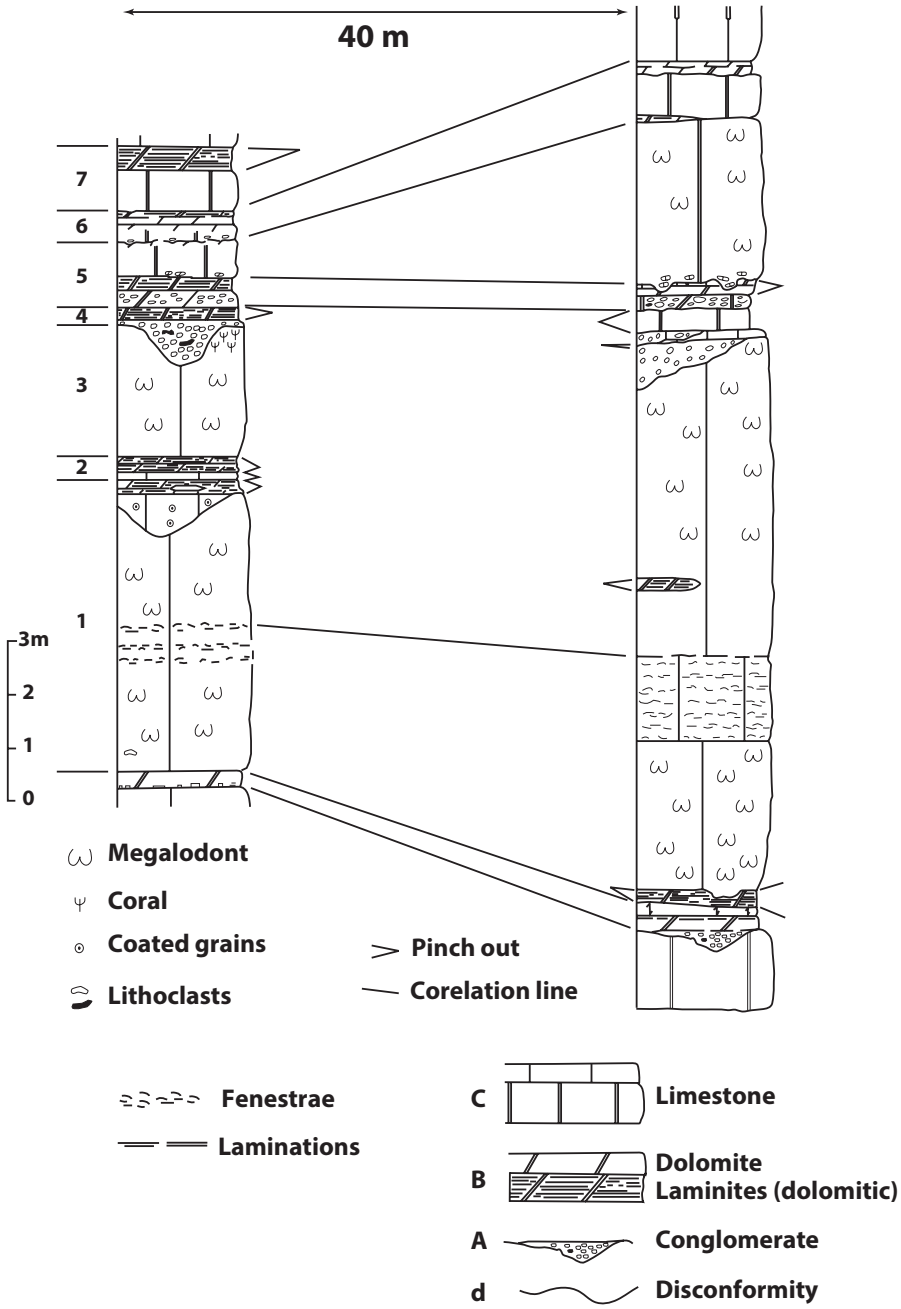

FIGURE 4 Laterally traced correlative intervals show the lateral variability among beds; Steinernes Meer section, 187–200 m. Lithologic designations A, B and C in legend follow the definitions of Fischer (1964; Figure 3). Member C is subdivided into wackestone/mudstone (lower bed; double vertical lines) and packstone/grainstone (upper bed). Cycles are delineated in the left margin. Numbers 1,2, 6 and 7 are C-B couplets that would be interpreted as shoaling upward by most sedimentologists. However, 1, 2 and 7 could logically be started with the underlying B interval, thus interpreted as 'deepening upward', that is, incomplete Fischer cycles; they are designated here as 'couplets', without a depth vector. The base of cycle 1 can be drawn with confidence only by tracing it laterally (right column) into a more distinctive B interval. This cycle could be broken into two at the fenestral interval or definitively into two (or three) with the appearance of a B interval in the right column. The channel form at top of the C interval (left column only) is filled with ooids, so is not considered a cycle-bounding disconformity. Cycle 3 is 'truncated', Cd. Cycle 4, dAB, is incomplete; it is classified as 'truncated, deepening' (Table 3). Cycle 5, ABCd?, has a deepening vector, as in Fischer's idealized cycle. However, in the right column, the correlative succession is A***BA***dCB, and the italicized *BA* couplet disappears further to the right. Cycle 6 has a possible disconformity at the base (not evident in the right-hand section), so it would be interpreted as shoaling upward. Several more cycle contrasts can be identified between the left and right columns, aided by the 'pinch out' symbols. The lateral variability between the two sections is unusual, even for Steinernes Meer. As a result, cycles would be interpreted quite differently in the right-hand section, and correlations between the two sections, only 40 m apart, would be problematic if based on cycle stratigraphy (or lithostratigraphy) alone

TABLE 1 Distribution of lithologies, Steinernes Meer, all units

Facies	Shale	Palaeosol[a]	Tidal	Subtidal
Fischer member		**A**	**B**	**C**
Number of beds	4	75	200	358
Percent of total	0.6	11.8	31.4	56.2
Mean thickness (cm)	122.4	15.7	26.5	235.0
Maximum thickness (cm)	250.5	130	180	2,890
Median thickness (cm)	110	10	19	110
Percent total thickness	0.5	1.3	5.8	92.3
Total number of beds = 637				

[a]Sixty-five additional discontinuities, not associated with palaeosols, were recorded.

5.8% of the total thickness. Discontinuous reddish, brown, yellow or grey argillaceous lime conglomerate, breccia or mudstone (Figure 2D and E) is 'member A', interpreted as palaeosol (Fischer, 1964). It accounts for 12% of the beds and 1.3% of the thickness. Fischer (1964, p. 113, 119) also included disconformities (d) in his ideal cyclothem, a useful distinction that most subsequent workers have overlooked (notable exceptions are Haas, 2004; Haas, Lobitzer, & Monostori, 2007). Conglomeratic palaeosols obviously involve disconformity, but others are defined by palaeokarst surfaces (Figure 5A) or by prominent, red-stained partings underlain by numerous sediment-filled vugs. The Steinernes Meer section includes 65 such surfaces. Red shales, confined to the non-cyclic interval, are volumetrically negligible at 0.6%. Mean bed thickness is 235 cm for members C, 26.5 cm for members B and 15.7 cm for members A (Table 1).

4.1 | Cycles

Cycles may be simply defined, following Bosence et al. (2009, p. 392), as repeated metre-scale sedimentary successions. The cycle boundary is taken as a pronounced erosion surface or a non-Waltherian facies shift. Inherent in the Waltherian criterion is a vector, that is, a shoaling or deepening succession. Such a vector is best defined by three or more elements; in Fischer's terms, ABC, CBA, CBd, etc. Among the various successions of beds in the Dachstein, the most common is alternating B and C members (Figure

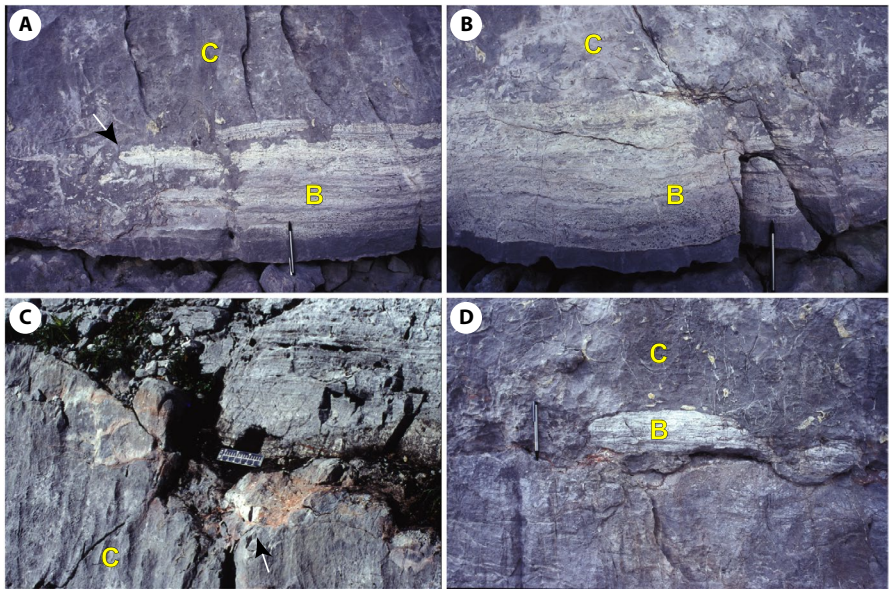

FIGURE 5 (A) and (B) Examples of pinchouts and reworking. An intertidal, whitish B horizon, underlying a subtidal, grey C member is well-developed in (B), but pinches out, by chemical erosion, in (A) (arrow). The breccia to the left in (A) is a soilstone, filling the resulting solution pit, which extends into the underlying subtidal limestone. A shallower solution pit is visible at the right of (B). This CBA-C succession defines a shallowing-upward cycle. Steinernes Meer section, 594.6 m. (C) Reddish lens of a palaeosol (A member, arrow) and clast of intertidal B member (whitish) preserved only in karst pockets atop a subtidal member C. (D) Whitish clast of laminated, dolomitic member B reworked into the base of a grey, subtidal C member. Pen in A, B and D is approximately 15 cm long. Scale in C is in centimetres and inches, foreshortened by the angle of view

4) without an intervening palaeosol (A) or disconformity (d). Such couplets have been routinely, uncritically, interpreted as 'shoaling up' CB cycles. However, without the vector provided by a disconformity or palaeosol, they could equally well be regarded as BC cycles, that is, deepening upward, or as symmetric CBC, with both deepening and shoaling components (cf. Enos & Samankassou, 1998, p. 220). Such alternations that lack a definitive vector are termed couplets here, rather than cycles. Goldhammer et al. (1990, pp. 552–553) subdivided B members into B1 and B2, corresponding to Fischer's 'algal-mat loferite' and 'pellet & homogeneous loferite' respectively, which they interpreted as 'upper supratidal' (B1) and 'intertidal' (B2). This relevant distinction could give a vector to the couplets defined here; CB2B1C would represent upward shoaling followed by an abrupt deepening. CB1B2C would represent a non-Waltherian shift, followed by a deepening sequence. However, the B1/B2 distinction did not prove very useful, as some lateral transitions exist between the two, and many B members have repeated fluctuations between B1 and B2 (e.g. beds 6 and 24, Figure 6A). Goldhammer's informal dictum that all cycles, no matter how small, must be honoured, is eminently reasonable where A, B and C members are involved. However, applying it rigorously to B1 and B2 intervals would involve, for example, dividing a bed 70 cm thick (#24, Figure 6A) into three cycles, each deepening upward. Such alternations are considered here as minor couplets, superposed on a larger scale CB couplet.

The section measured at Steinernes Meer includes the upper 885 m of the Dachstein, up to the contact with the Jurassic Knollenkalk. The lower 611 m contains 222 peritidal cycles and couplets. The overlying 199 m is largely non-cyclic subtidal deposits, including a few intervals of reddish shale and lime mudstone, as well as thickets of arborescent corals and beds of oolite. The uppermost 74 m of the Dachstein is weakly cyclic, with 24 cycles and couplets. Fischer (1964) measured 120 m at Steinernes Meer containing 20 cycles, Goldhammer et al. (1990) measured 192 m including 61 cycles near the base of the section of the present study, and Satterley (1996b) measured the top 716 m of the Dachstein, but did not specify the number of cycles encountered. The last two studies each concluded that the cycles were shoaling upward, in opposition to Fischer's 'typical Lofer cycle'. Studies of the Dachstein elsewhere have concluded that the famous cycles are shallowing upward (Cozzi, Hinnov, & Hardie, 2005, Julian Alps, Italy), deepening upward (Borza, 1977, Muránskej planiny, Slovakia; Haas, 1982, 1991, Transdanubian Range, Hungary) or 'essentially symmetric' (Haas, 1994, Transdanubian Range). Haas (1991) detailed the considerable complexity of the Dachstein cycles. Fischer noted, 'There are many different cycles in the Dachstein that I could have chosen, but I picked the deepening upward' (A.G. Fischer, letter of 2 October 1997). Despite this disclaimer, all of the cycles illustrated by Fischer (1964, his figs 3, 4, 6 and 38) were interpreted as deepening upward.

4.2 | Continuity of beds

Lateral continuity, or the lack thereof, is another salient feature of the Dachstein in Steinernes Meer (cf. Satterley, 1996b), Loferer Steinberge, and elsewhere in the Northern Limestone Alps (Piller, 1976, 1981; Zankl, 1967). This is documented in the Steinernes Meer section: of 558 subtidal and peritidal beds measured, 121 (21.6%) disappear laterally (Table 2, Figures 4 and 5A through D). The distinctive B (peritidal) intervals account for 74% of the disappeared, corresponding to 45% of the total peritidal beds. Subtidal C horizons comprise 26% of the disappeared; this is 8.9% of the total subtidal beds. Disappearances westward, toward the inferred platform interior, are 10.0% of all beds. Eastward toward the platform margin, 11.6% of the beds disappear (Table 2). A large portion of this variability arises from erosion of the distinctive tidal deposits. This can result in the apparent merger of two C beds; unless some clasts mark the eroded interval, erosional horizons are rarely detectable. Most palaeosol A members disappear within the outcrop, but many reappear sporadically where the horizon is traced laterally (Figure 5C). The discontinuity percentages would be much higher, but less meaningful, if A beds were included.

Another aspect of lateral variability is marked changes in thickness. Seventy three beds, 13.1% of the total peritidal and subtidal beds, show lateral variations in thickness greater than 10%, despite limited lateral exposure (Table 2). Mean thickness variation is 49%. Of beds with thickness changes, 27% are peritidal and 73% subtidal horizons, representing 9.5 and 15%, respectively, of that bed type (Table 2). Significant thinning was measured in 6.5% of beds westward toward the platform interior and 6.6% toward the margin. There is little indication of compensation between thickness changes. In the relatively few cases where adjacent beds both showed significant thickness changes, 11 were in opposite directions (compensatory?) and eight were in the same direction. Moreover, six of the instances of opposing sense changes were between subtidal beds in non-cyclic intervals. Thus change in bed thickness generally means change in cycle thickness. As with disappearances, palaeosols were excluded from tabulation; probably 100% of such beds would show 100% variation in thickness, if traced laterally for as little as a few hundred metres.

Vanishing beds are twice as common in the cyclic lower Dachstein compared to the upper units (25.0% vs. 12.7%), reflecting the concentration of laterally discontinuous peritidal deposits within the cycles. In contrast, more lateral thickness variations were noted in the upper units (23.2% vs. 13.1%), in part because of the preponderance of more variable C beds (92% of B + C beds) in the non-cyclic unit. Another factor

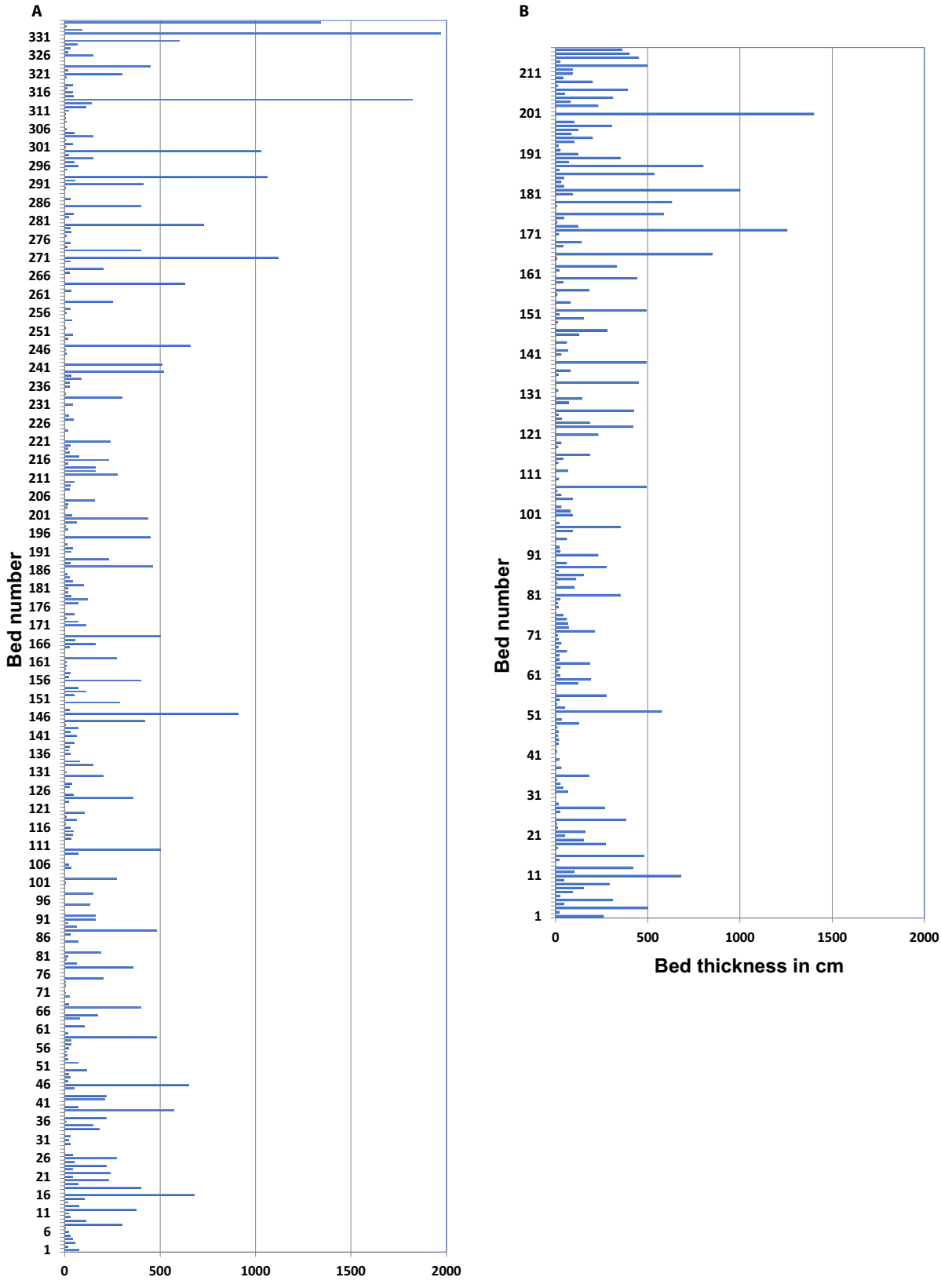

FIGURE 6 Bed thickness plots of Steinernes Meer section (A) versus Loferer Steinberge (B). (A) is from base to 350 m. Fischer plots (Figure 7) suggest that bed 262 at 216.5 m in Steinernes Meer, 6A, should approximately correlate with bed 157 at 145 m in Loferer Steinberge, 6B. These are at the minima in the respective Fischer plots. The adjacent beds cannot be readily correlated, nor can those at the secondary maxima and minima

was more extensive and accessible exposures in the upper section.

A more dramatic measure of lateral variability is provided by an offset of 1.7 km within the Steinernes Meer section from the vicinity of Breithorn to the Rotwandl trail. Distinctive features and sequences allowed correlation of the overlapping portions of the section. About 26 m of the overlap were measured, which incorporated 19 B and C beds. Of these, 11 disappeared and six others changed thickness significantly between sections. This small sample strongly suggests that with more extensive exposure, the statistics on variability would be substantially higher.

Comparing the Steinernes Meer and Loferer Steinberge sections provides a larger scale demonstration of variability. Steinernes Meer includes almost the complete Dachstein, so the strongly cyclic Loferer section must be equivalent to some part of the cyclic interval. 'Fischer plots', which portray some aspect of evolution of filled accommodation space as cumulative departures from mean cycle thickness (Fischer, 1964; Sadler, Osleger, & Montañez, 1993), suggest that the equivalency lies between 53 and 345 m in the Steinernes Meer section (cycles number 20 through 130, Figure 7). Comparisons of cycles within the two sections at the multiple maxima and minima of the plots failed to provide any acceptable correlations. Plots of variations in bed thickness (Figure 6) also failed to produce reliable correlations. Over a distance of 22 km, variations in bed and cycle character are such that not a single cycle can be reliably correlated. Schwarzacher (2005, p. 104) also compared a Fischer plot of the Steinernes Meer section with plots of his aerial-photo data from Loferer Steinberge and the intervening Leoganger Steinberge and similarly concluded, 'The curves suggest a similarity of sedimentation but the differences…are too large to be conclusive'.

5 | INTERPRETATION AND DISCUSSION

Fischer's (1964) seminal paper on 'Lofer cyclothems' is widely cited in reports of 'shoaling up cycles', abundant in platform carbonates, completely ignoring that his dABC cycle is deepening upward. Given the controversy about the nature of Dachstein cycles, close attention was paid to shoaling and deepening vectors. Of the 222 'cycles' identified in the lower 611 m of the measured Dachstein, 100 (45%) are CB/CB couplets, without a definitive shoaling or deepening vector (Table 3). A further 28.7% are incomplete because of truncation, typically by a conglomeratic palaeosol (A member) or microkarstic disconformity (d) overlying a subtidal C member, unequivocally indicating a relative drop in sea-level. Such truncated cycles are, curiously, sometimes called 'diagenetic' cycles (Bosence et al., 2009, p. 397, and references therein). Only 26.6% of cycles are relatively complete. Of these 4.5% are deepening upward,

TABLE 2 Lateral variability, Steinernes Meer, complete section

	West	East	Total
'Disappeared'			
Number of beds, B + C[a]	56	65	121
Percentage of all B + C[a]	10.0	11.6	21.6
Thinning of beds			
Number of beds	36	37	73
Percentage of all beds[a]	6.5	6.6	13.1
Mean thickness change (%)	49.2	49.3	49.2

Variability by facies	Tidal (B)	Subtidal (C)
'Disappeared'		
Number of beds	89	32
Percentage of all beds, B + C[a]	15.9	5.7
Percentage of bed type	44.5	8.9
Thinning		
Number of beds	19	54
Percentage of all beds[a]	3.4	9.7
Percentage of bed type	9.5	15.1
Total number of beds = 558		

[a]'A' beds (soil horizons) were not included in compilations. Their extreme lateral variability and discontinuity would inflate values and obscure the variability of the other lithologies.

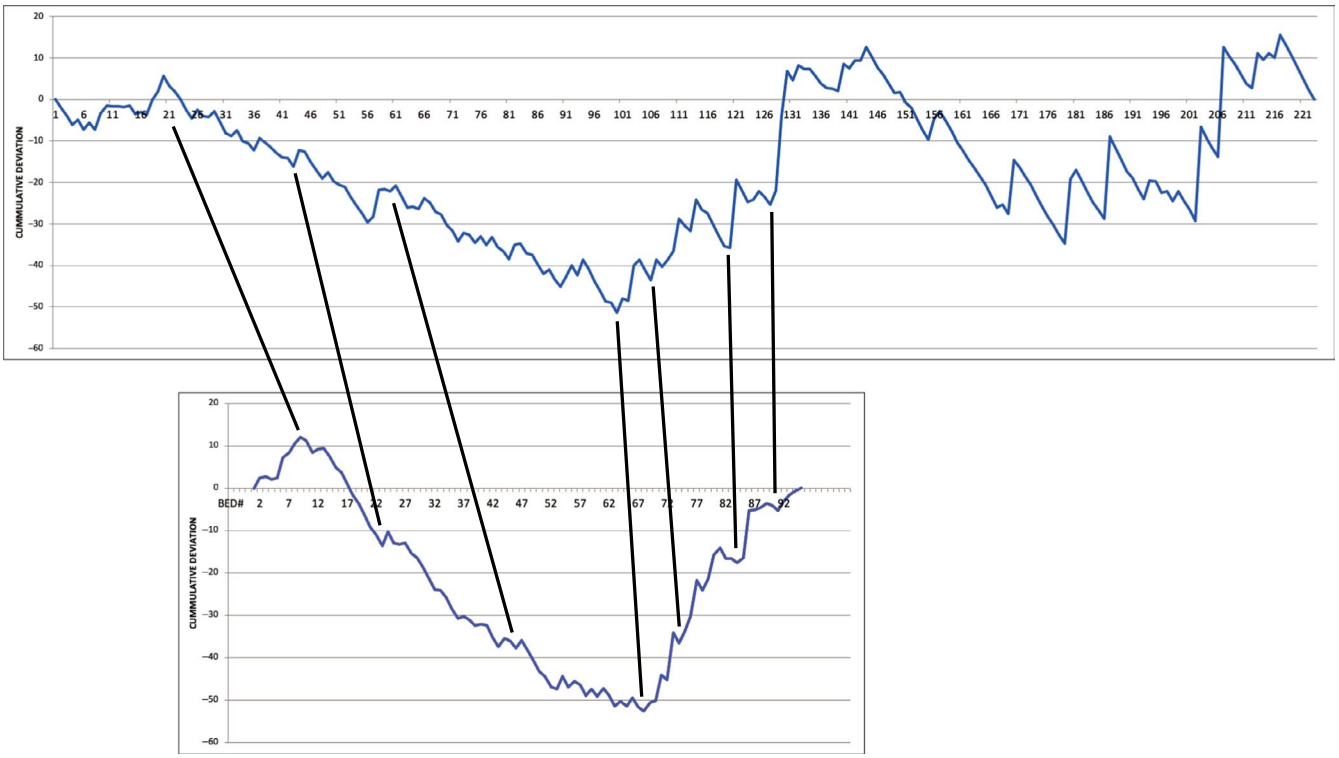

FIGURE 7 Fischer plots of the measured sections at Steinernes Meer (top, cyclic interval, 0–611 m) and Loferer Steinberge (below). Horizontal axes are cycle numbers, in sequence from the base of section. Vertical axes are cumulative deviation from mean cycle thickness (m). The curves are proxies for fluctuations in filled accommodation during successive high stands of sea level, assuming a constant rate of subsidence, because each cycle is terminated by reaching or crossing sea-level, represented by tidal deposits (member B), a palaeolsol (member A), or a subaerial disconformity (d). The plot of the Loferer Steinberge section has the general shape of the Steinernes Meer plot, cycles 18 through 129. This interval of 112 cycles in Steinernes Meer appears to correlate generally with the 95 cycles in Loferer Steinberge. The thickness of the intervals is 352 and 272 m respectively. However, none of the secondary maxima and minima, some of which are connected by straight lines, can be reliably correlated. With good correlations the lines should be approximately parallel. The two pairs on the right are nearly so, but note the contrasts in details of the two curves

for example, dABC. Symmetrical cycles, such as ABCBA, comprise 12% of the total and shoaling upward, for example, CBAd, 9.9%. In contrast, the 93-cycle Loferer Steinberge section with 28% 'complete' cycles has 11.8% deepening, 3.2% shoaling and 12.9% symmetrical (Table 3).

Before declaring a winner – or a draw – recall that 45% of the totals are CBCB couplets (and 49% in Loferer Steinberge section, Table 3), which many workers would uncritically consider to represent shoaling upward. Most of the cycles (26% and 20%) truncated by subaerial exposure could also be considered shoaling upward; they clearly represent a drop in relative sea level. These generalizations would give shoaling-up cycles – and fragments – an overwhelming 81% majority in Steinernes Meer and 73% in Loferer Steinberge. By any

'COMPLETE' CYCLES			TRUNCATED CYCLES		COUPLETS
Deepening	**Shoaling**	**Symmetrical**	**Deepening**	**Shoaling**	
dABC	CBAd	ABCBA	dAC	Cd	CBCB
Steinernes Meer, cyclic interval ($N = 222$)					
4.5	9.9	12.2	2.7	26	45
Loferer Steinberge ($N = 93$)					
11.8	3.2	12.9	2.2	20.4	49.4
Steinernes Meer, Fischer A compliant ($N = 247$)					
10.9	6.5	14.6	5.3	35.2	27.5

Values are percentages. Cycle types listed are representative of many variants.

TABLE 3 Cycle census, Steinernes Meer cyclic interval (0–611 m, top), Loferer Steinberge (middle), and Steinernes Meer (0–611 m, bottom), using strict Fischer definition of Member A

accounting, Fischer's ideal Lofer cycles are a small minority, 4.5%–10.9%.

How did Fischer decide on the deepening upward ABC sequence as the typical Lofer cyclothem? The fine print of Fischer's (1964) treatise clarifies that he defined member A very much on lithology rather than stratigraphy: 'In many instances it is merely a shaly bedding plane; in many others it is entirely restricted to cavity fillings…. It also forms most of the neptunian dikes'. (p. 121). A re-evaluation of the Steinernes Meer cyclic section employing this concept increased the number of A members from 59 to 130 and subdivided 11 thick C members at partings subtended by numerous vugs reduced by red internal sediment. This obviously altered the cycle census, increasing the number to 247 and the deepening upward percentage from 4.5 to 10.9, while reducing the shoaling upward tally from 9.9% to 6.5% (Table 3). Moreover, most of the 'symmetrical' cycles are skewed toward the deepening limb, typically ABCB. These numbers and the Loferer Steinberge percentages may elucidate why Fischer chose the deepening ABC sequence as typical for the Dachstein.

This approach may produce a more realistic understanding of cycle character than does identifying major breaks solely by conglomeratic palaeosols, as initially assessed here (Table 3, top) and by others (cf. Goldhammer et al., 1990, p. 552). However, some 'shaly bedding planes' may be stylocumulates (Enos & Samankassou, 1998, p. 214), and some of the red internal sediment derives from nearby neptunian dikes rather than an immediately overlying exposure surface (Enos & Samankassou, 1998, p. 218). The actual number of breaks in sedimentation accompanied by subaerial weathering probably lies somewhere between the 65 and 130 estimated employing the two criteria for recognition.

Dachstein cycles, like most others in shallow platform carbonates, have commonly been interpreted to reflect eustatic sea-level changes (summarized by Enos & Samankassou, 1998). Both the variety of cycles (Table 3) and the marked lateral discontinuity of beds (Table 2) suggest other processes were involved as well. These could be allogenic, autogenic or random stacking. Perhaps the most thorough investigation of the 'Diktators' of peritidal carbonate cycles to date was by Bosence et al. (2009) on the Liassic platforms of western Tethys. They concluded that the stacking pattern of Liassic facies (but not of cycles) is definitely non-random (p. 406), and that the main driver was pulsed tectonic subsidence. They acknowledge, however, that both eustasy and autocyclicity may also have influenced cycle formation, stating, 'There are no known criteria available to sedimentologists to recognize such combinations of cycle-forming processes'. Against this backdrop (see also Hill, Wood, Curtis, & Tetzlaff, 2012), it may be unrealistic to explore further the origin of Lofer cycles based on a comparatively small data set, but the question should at least be framed.

If the cycles resulted exclusively from eustatic (allocyclic) forcing, cycles should be synchronous and continuous across platforms (cf. Goodwin & Anderson, 1985; Read & Goldhammer, 1988) or even between basins (Osleger, 1991b; Osleger & Read, 1991). Individual Steinernes Meer cycles and couplets cannot be correlated with Lofer Steinberge, 22 km distant on the same platform (Figure 7; Schwarzacher, 2005, fig. 11). Other processes apparently played a significant role in cycle formation or modification.

Rare intervals of red marine shale and reddish lime mudstone in the non-cyclic Dachstein interval indicate rapid deepening of appreciable magnitude ('Kössen events') driven by short-term syndepositional tectonic movements (Satterley, 1996a & b) or rapid rises in sea level. The thickening of subtidal beds toward the top of the cyclic section, indicated by Fischer plots (Figure 7), suggests a long-term deepening trend as well. Late Triassic (Norian) long-term extensional tectonics at the margins of Tethys (Bernoulli & Jenkyns, 1974) may have affected the Dachstein area, as suggested by Satterley (1996a). Tectonics may thus have influenced the evolution of the Dachstein platform, specifically by creating or contributing to accommodation space that allowed accumulation of shales, thick cycles and extended subtidal intervals higher in section.

A fall in relative sea level, whether eustatic or tectonic, is required to superpose subaerial exposure features on subtidal facies, so-called diagenetic cycles, observed in a quarter of the Dachstein cycles. This cannot be autocyclic.

Lateral variations in thickness can be readily explained by differential sedimentation rates, as commonly documented in Holocene sediments (Bosence, 2008; Eberli, 2013; Enos & Perkins, 1979; Harris et al., 2011; Purkis & Harris, 2016; Wilkinson & Drummond, 2004). This is an autocyclic process, albeit not one that is likely to independently generate cycles. One could also question how relevant observations from a single, incomplete cycle in an icehouse Earth are to the Late Triassic, but surely differential sedimentation has existed throughout geologic time.

Ginsburg (1971) suggested that autogenic processes alone could generate shallowing-upward cycles through progradation of tidal flats. This model requires (a) general long-term subsidence (Cowan & James, 1996), necessary for any thick shallow-water accumulation and (b) lag time (or 'lag depth', Enos, 1989), a necessary condition to generate repetitive shoaling cycles in any model. Ginsburg's model has been widely invoked (cf. Bosence et al., 2009; Burgess, 2006; Burgess & Wright, 2003; Burgess et al., 2001; Goldhammer, Lehmann, & Dunn, 1993; Hardie & Shinn, 1986), as well as questioned (Koershner & Read, 1989, p. 674; Goldhammer et al., 1993, p. 340; Zühlke, 2004, p. 201; Schwarzacher, 2005, p. 105). Much credence in the model has derived from computer simulations (Burgess & Wright, 2003; Burgess et al., 2001; Goldhammer et al., 1993; Hill et al., 2012).

Various other intrinsic processes have been proposed to explain peritidal cycles (Table 4). Objections that autocyclic processes lack a feedback mechanism to start or restart a cycle (cf. Schwarzacher, 2005, p. 105) ignore the potential of erosion by storms or channels to create an erosive surface and initiate a new shoaling sequence. Wanless (1979) identified wedges of mud 1.5 m thick that compose up to 70% of a Florida Bay mud bank and provided evidence of sedimentation by a single 'super hurricane'. Less catastrophically, migration of a tidal channel could erode a cycle partially or entirely and initiate deposition to form a new shoaling-up sequence relatively rapidly (Cloyd et al., 1990). Satterley (1996b) proposed such a mechanism to explain lateral variations within the Dachstein in Steinernes Meer.

Erosion of peritidal intervals was a common process in the Dachstein, readily documented by lateral truncation and reworking of distinctive dolomitic, laminated peritidal lithoclasts into overlying or laterally equivalent subtidal facies (Figure 5A and B) or into a conglomeratic soilstone (Figures 2E and 5C). Perhaps more common is chemical erosion to produce microkarst surfaces, which can completely truncate thin tidal intervals (Figure 5A and B) or preserve only clasts in microkarst pockets (Figure 5C). More gradual lateral thinning of beds suggests differential production or transport and redistribution of sediment, important factors in progradation of modern tidal flats (Ginsburg, 1971; Hardie & Shinn, 1986). Such differential accumulation was apparently active in the Dachstein platform, as proposed by Satterley (1996b), and indicated by the facies mosaic reported by Zankl (1967) and Piller (1976, 1981). Similar mosaics are demonstrated by Holocene examples (cf. Eberli, 2013; Enos & Perkins, 1979; Rankey, 2002; Wilkinson & Drummond, 2004; Yang, Mazzullo, & Teal, 2004), as well as many older deposits (Cowan & James, 1996; Eberli, 2013; Laporte, 1967; Pratt & James, 1986). Thus, intrinsic, autocyclic processes, erosion, transport and non-uniform distribution of sediments, presumably superposed on stratigraphic sequences driven by eustasy and subsidence, led to the complex pattern of cycles recorded in the Dachstein.

Fischer noted 'many different cycles in the Dachstein' (A.G. Fischer, letter of 2 October 1997). Haas (1982) reported complex cycles in the Dachstein from Hungary. Autocyclic overprinting most likely masked the primary eustatic signals to produce chaotic cycle patterns (Table 3). Seemingly Poisson distribution is reported from other Phanerozoic platforms (Algeo & Wilkinson, 1988; Dietrich & Wilkinson, 1999; Wilkinson, Drummond, Diedrich, & Rothman, 1997), modern examples (Rankey, 2002) and platform modelling (Burgess, 2001; Burgess & Wright, 2003; Burgess et al., 2001). Obviously, mosaic facies distribution in carbonate platforms deposits is not unique to the Dachstein nor to the Triassic. Autocyclic processes tend to produce gentle nudges rather than strong forcing, so presumably they had more impact during a greenhouse Earth (such as the Triassic), with relatively low-amplitude, short-period cyclicity. In contrast, the eustatic Diktator would dominate in an icehouse world (cf. Read, 1995; Wright, 1992).

The original 'Fischer plot' was constructed from a short section (120 m; 20 cycles) in Steinernes Meer (Fischer, 1964, fig. 38), and the resulting curve attributed to variations in the rate of subsidence. This construction was resurrected and modified by Goldhammer et al. (1987) and interpreted as a

TABLE 4 Proposed autocyclic mechanisms

Reference	Process	Example
Algeo and Wilkinson (1988)	Fluctuations in sediment production 'Vagaries' in sediment deposition	Phanerozoic strata, various lithologies and depositional environments
Cloyd et al. (1990)	Tidal-channel migration	Waterfowl Fm. (Cambrian) Alberta, Canada
Cowan, and James (1996)	Tidal-flat island migration	Cambrian, Newfoundland, Canada
Drummond and Dugan (1999)	Self organization	Computer simulation
Ginsburg (1971)	Tidal-flat progradation	Andros Island (Holocene), Bahamas
Osleger (1991a)	Wave sweeping (erosion)	U. Cambrian, House Range, Utah, USA
Peper and Cloetingh (1995)	Slope instability	Computer simulation
Pratt and James (1986)	Tidal-flat island migration	St. George Grp. (Ordovician) Newfoundland, Canada
Satterley (1996b)	Tidal-channel migration	Dachstein Fm. (U. Triassic) Steinernes Meer, Austria
Spencer and Demicco (1989)	Local isostatic subsidence Differential sediment production and distribution Differential compaction	Computer simulation
Wanless (1981)	Storm erosion, grass-bed migration	Holocene, south Florida, USA
Wilkinson et al. (1997)	Random stacking, biological mediation	Kinblade & West Spring Creek Fms. (Ordovician) Arbuckle Mtns, Oklahoma, USA

record of eustasy within the Milankovich interval. Such plots have subsequently been extensively used, purporting to depict third-order fluctuations in sea-level (Read & Goldhammer, 1988), oscillations in sea level in subtidal cycles (Osleger & Read, 1991), variations in accommodation space (Bosence et al., 2009; Goldhammer et al., 1993; Husinec, Baschb, Rose, & Read, 2008), variations in filled accommodation space, deviation from expected cycle behaviour (warped into the depth domain; Day, 1997), etc. Criticism of such interpretation has followed apace (Boss & Rasmussen, 1995a, 1995b; Burgess & Wright, 2003; Eberli, 2013). Objectively, Fischer plots simply display cumulative departure from mean cycle thickness (Sadler et al., 1993).

It is beyond the scope of this study and the authors' expertise to settle this controversy, but it is possible to address the failure in correlation between sections in Steinernes Meer and Loferer Steinberge using Fischer plots (Figure 7). It was not possible to establish any correlations between individual cycles from the thickness or character of the cycles at secondary maxima and minima in the two Fischer plots. This apparently results from lateral changes in the cycles, including the disappearance of any record of some entire cycles, owing primarily to physical and chemical erosion of peritidal caps. This in turn illustrates an inherent weakness in Fischer plots for comparing sections with significant lateral variability. The comparative Fischer plots in Figure 8 illustrate a related weakness. The lower plot containing the 'disappeareds' differs significantly from the plots that represent an extreme case of a core or a linearly measured section ignoring lateral variations. Those plots have a different average thickness because of amalgamations, but more importantly display abrupt thickening of a few cycles and long intervals of thinner 'normal' cycles, introducing artefacts that could produce erroneous interpretations and correlations – or lack thereof.

The numerous lateral variations in individual Dachstein cycles would complicate spectral analysis of the thickness patterns, typically conducted in search of 'Milankovich frequencies'. Random lateral variations would be more troublesome than the 'missed beats' produced by long-period eustatic fluctuations that are expressed as anomalously thick subtidal beds (high sea-level) or amalgamated tepee intervals (low sea level; Goldhammer et al., 1990). Lateral variations may lead to 'spatio-temporal masking' (Tipper, 1998) in data from sections or wells, a potential source of error in sea-level reconstructions and cyclostratigraphy. Lateral variations certainly must complicate the quest for orbital parameters at its birthplace in the Dachstein.

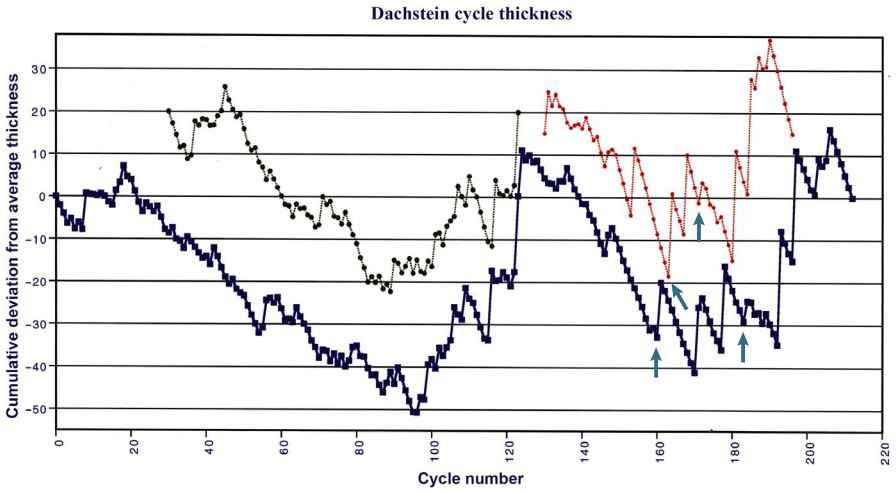

FIGURE 8 Fischer plot showing deviations from mean cycle thickness of the cyclic portion (0–611 m) of the Steinernes Meer measured section. The lighter plots above (in colour) are of the same section with all of the beds that laterally disappear removed and the cycles redefined accordingly. Lateral changes in bed thickness do not affect cycle numbers, so they were not incorporated, although they would further differentiate the plots. Rather than starting these two plots at zero, they are tied to 20 m (lower portion) and 15 m (upper portion) to prevent overlap of the plots. The 'disappeareds' plots are, of course, shorter because of the merged cycles, generally where a peritidal B interval disappears. These plots represent an extreme case of a linearly measured section, with no lateral control, or of a core. The disappearance of the B members, observed from lateral tracing, produced thick, amalgamated cycles. The resulting, apparently asymmetric, 'megacycles' could lead to erroneous interpretations. If the lateral variations are ignored, abrupt thickening of a few cycles would be interpreted as a rapid rise of relative sea-level (or tectonic subsidence) and long intervals of thinner 'normal' cycles as a sea-level fall that decreased the accommodation. These plots thus include artefacts, misleading for correlation and violations of the assumption that cycles are of equal duration (Fischer, 1964). Although the general shapes of the curves are similar, individual beds could scarcely be correlated with confidence, despite representing the same sequence of rocks from the same measured section. Note, for example, that the three positive spikes between cycles 160 and 183 (arrows) are reduced to two in the upper plot (between 163 and 171, arrows) and that the number of apparent cycles is reduced from 24 to 9. Recall that these plots represent the same interval of rocks, with the cycles altered only by the disappearance of beds

Schwarzacher (1954) and Fischer (1964) both speculated about orbital influence on sedimentation. However, spectral analysis of a short section from Steinernes Meer (192 m, 61 cycles) detected no discernible vertical stacking pattern (Goldhammer et al., 1990, p. 554). Schwarzacher (2005, p. 101) produced a power spectrum of the Steinernes Meer section of the present study in the thickness domain, but did not attempt to convert it to time.

Controversy about cycle duration extends well beyond the Dachstein platform. Cycles of the Middle Triassic Latemar platform, presented as a prime example of Milankovitch-driven cycles (Goldhammer et al., 1987), are currently a matter of intense debate (see Brack, Mundil, Oberli, Meier, & Rieber, 1996; Cozzi et al., 2005; Forkner, Hinnov, Goldhammer, & Hardie, 2009; Hinnov, 2006; Kent, Muttoni, & Brack, 2004; Mundil et al., 2003; Preto, Hinnov, De Zanche, Mietto, & Hardie, 2004; Spahn, Kodama, & Preto, 2013; Zühlke, 2004; Zühlke, Bechstadt, & Mundil, 2003). If comparable lateral variations occur in other platforms, and there is little reason to doubt that they do (cf. Eberli, 2013), autogenic processes deserve more consideration and detailed critical analysis. The three orbital cycles noted by Milankovitch (1941) should converge to reduce solar radiation below the critical threshold for glaciation, and consequent sea-level fluctuations, only periodically during geological time (Berger, 1988). The Late Triassic may not have been one of those epochs.

Signals deduced from a typical measured section must represent a composite of intrinsic and allocyclic factors, so should not be uncritically interpreted (or rejected) as eustatic signals (see also Peper & Cloetingh, 1995; Wilkinson et al., 1997). As allocycles should be synchronous and continuous across facies belts (cf. Goodwin & Anderson, 1985; Osleger & Read, 1991; Read & Goldhammer, 1988), lateral tracing as quantified here should underpin cyclostratigraphy. Incorporating all lateral variations into a composite sequence will result in the most complete section possible, surely a prerequisite for well-founded interpretations of whatever kind.

6 | CONCLUSIONS

The Dachstein limestone at Steinernes Meer includes 222 peritidal cycles in the basal 611 m, including shoaling and deepening upward, symmetrical, and truncated cycles, as well as 'couplets' without a depth vector. Dachstein cycles demonstrably record relative sea-level changes, that is, subtidal deposits truncated by soilstone, but the lack of lateral continuity of beds and cycle-bounding surfaces is consistent with an autocyclic component to stratification. Physical and chemical erosion of intertidal intervals is the most readily documented process producing lateral discontinuity and amalgamation of cycles. Non-uniform rates of production, transport and distribution of sediment, superposed on eustasy, probably also contributed to the complex cycle patterns recorded in the Dachstein. Extensive lateral facies variations, which are not unique to the Dashstein, limit the utility of Fischer plots in such sequences. The quest to extract Milankovitch frequencies from platform carbonates may also be compromised by these changes in cycle character.

ACKNOWLEDGEMENTS

We gratefully acknowledge the logistic help of Beate Fohrer and the hospitality of the crew of Manfred Gruber, Jr. at Riemannhaus and Katharina Filzer-Meiberger at von-Schmidt-Zabierow Hütte. A critique from Gregor Eberli led to significant improvements in our opus. E.S. benefited from the financial support of the Deutsche Forschungsgemeinschaft (German Research Foundation, grant FL 42/81) and of the Swiss Science Foundation. P.E. was supported by the van Sant Fund and Haas Fund, University of Kansas. The late Robert N. Ginsburg introduced P.E. to carbonate sedimentation in 1964-1965 and mentoring continued during co-led field trips (1976–1980) and a post-doc stint (2007–2010) at the Comparative Sedimentology Laboratory.

DATA AVAILABILITY STATEMENT

The data that support the findings of this study are available from the corresponding author upon reasonable request.

ORCID

Elias Samankassou https://orcid.org/0000-0003-0385-7686

REFERENCES

Adams, R. D., & Grotzinger, J. P. (1996). Lateral continuity of facies and parasequences in Middle Cambrian platform carbonates, Carrara Formation, southeastern California, U.S.A. *Journal of Sedimentary Research*, *66*, 1079–1090.

Algeo, T. J., & Wilkinson, B. H. (1988). Periodicity of mesoscale Phanerozoic sedimentary cycles and the role of Milankovitch orbital modulation. *Journal of Geology*, *96*, 313–322.

Bádenas, B., Aurell, M., & Bosence, D. (2010). Continuity and facies heterogeneities of shallow carbonate ramp cycles (Sinemurian, Lower Jurassic, North-east Spain). *Sedimentology*, *57*, 1021–1048.

Beerbower, J. R. (1964). Cyclothems and cyclic deposition mechanisms in alluvial plain sedimentation. In D. F. Merriam (Ed.), *Symposium on cyclic sedimentation*. *Kansas Geological Survey Bulletin*, *169*, 31–41.

Benedictis, D. D., Bosence, D., & Waltham, D. (2007). Tectonic control on peritidal carbonate parasequence formation: An investigation using forward tectono-stratigraphic modeling. *Sedimentology*, *54*, 1–19.

Berger, A. (1988). Milankovitch theory and climate. *Reviews of Geophysics*, *26*, 624–657.

Bernoulli, D., & Jenkyns, H. C. (1974). Alpine, Mediterranean, and central Atlantic Mesozoic facies in relation to the early evolution of the Tethys. InR. H. Dott, & R. H. Shaver (Eds.), *Modern and ancient*

geosynclinal sedimentation. *Society of Economic Paleontologists and Mineralogists, Special Publication*, *19*, 129–160.

Borza, K. (1977). Cyklická sedimentácia dachsteinskych vápencov Muránskej planiny. *Geologické Pracé, Bratislava*, *67*, 23–52.

Bosellini, A. (1967). La tematica deposizionale della Dolomia Principale (Dolomiti e Prealpi Venete). *Bollettino della Società Geologica Italaliana*, *86*, 133–169.

Bosence, D. (2008). Randomness or order in the occurrence and preservation of shallow-marine carbonate facies? Holocene, South Florida. *Palaeogeography, Palaeoclimatology, Palaeoecology*, *270*, 339–348.

Bosence, D., Procter, E., Aurell, M., Kahla, A. B., Boudagher-Fadel, M., Casaglia, F. … Waltham, D. (2009). A dominant tectonic signal in high-frequency, peritidal carbonate cycles? A regional analysis of Liassic platforms from Western Tethys. *Journal of Sedimentary Research*, *79*, 389–415.

Boss, S. K., & Rasmussen, K. A. (1995a) Misuse of Fischer plots as sea-level curves. *Geology*, *23*, 221–224.

Boss, S. K., & Rasmussen, K. A. (1995b). Misuse of Fischer plots as sea-level curves: Comment and reply. *Geology*, *23*, 1049–1050.

Brack, P., Mundil, R., Oberli, F., Meier, M., & Rieber, H. (1996). Biostratigraphic and radiometric age data question the Milankovitch characteristics of the Latemar cycles (Southern Alps, Italy). *Geology*, *24*, 371–375.

Burgess, P. M. (2001). Modeling carbonate sequence development without relative sea-level oscillations. *Geology*, *29*, 1127–1130.

Burgess, P. M. (2006). The signal and the noise: Forward modelling of allocyclic and autocyclic processes influencing peritidal stacking patterns. *Journal of Sedimentary Research*, *76*, 962–977.

Burgess, P. M. (2016). Identifying ordered strata: Evidence, methods, and meaning. *Journal of Sedimentary Research*, *86*, 148–167.

Burgess, P. M., & Wright, V. P. (2003). Numerical forward modeling of carbonate platform dynamics: An evaluation of complexity and completeness in carbonate strata. *Journal of Sedimentary Research*, *73*, 637–652.

Burgess, P. M., Wright, V. P., & Emery, D. (2001). Numerical forward modeling of peritidal carbonate parasequence development: Implications for outcrop interpretation. *Basin Research*, *13*, 1–16.

Celarc, B., Gale, L., & Kolar-Jurkovšek, T. (2014). New data on the progradation of the Dachstein carbonate platform (Kamnik-Savinja Alps, Slovenia). *Geologija*, *57*, 95–104.

Cisne, J. L. (1986). Earthquakes recorded stratigraphically on carbonate platforms. *Nature*, *323*, 320–322.

Cloyd, K. C., Demicco, R. V., & Spencer, R. J. (1990). Tidal channel, levee, and crevasse-splay deposits from a Cambrian tidal channel system: A new mechanism to produce shallowing-upward sequences. *Journal of Sedimentary Research*, *60*, 73–83.

Cowan, C. A., & James, N. P. (1996). Autogenic dynamics in carbonate sedimentation: Meter-scale, shallowing-upward cycles, Upper Cambrian, Western Newfoundland, Canada. *American Journal of Science*, *296*, 1175–1207.

Cozzi, A., Hinnov, L. A., & Hardie, L. A. (2005). Orbitally forced Lofer cycles in the Dachstein Limestone of the Julian Alps (northeastern Italy). *Geology*, *33*, 789–792.

Day, P. I. (1997). The Fischer diagram in the depth domain: A tool for sequence stratigraphy. *Journal of Sedimentary Research*, *67*, 982–984.

Demicco, R. V. (1985). Platform and off-platform carbonates of the Upper Cambrian of western Maryland, U.S.A. *Sedimentology*, *32*, 1–22.

Dietrich, N. W., & Wilkinson, B. H. (1999). Depositional cyclicity in the Lower Devonian Helderberg Group of New York State. *The Journal of Geology*, *107*, 643–658.

Drummond, C. N., & Dugan, P. J. (1999). Self-organizing models of shallow-water carbonate accumulation. *Journal of Sedimentary Research*, *69*, 939–946.

Eberli, G. P. (2013). The uncertainties involved in extracting amplitude and frequency of orbitally driven sea-level fluctuations from shallow-water carbonate cycles. *Sedimentology*, *60*, 64–84.

Egenhoff, S. O., Peterhänsel, A., Bechstädt, T., Zühlke, R., & Grötsch, J. (1999). Facies architecture of an isolated carbonate platform: Tracing the cycles of the Latemar (Middle Triassic, northern Italy). *Sedimentology*, *46*, 893–912.

Enos, P. (1989). Lag time – Is it simply storm wave base? In E. K. Franseen, & W. L. Watney (Eds.), *Sedimentary modelling: Computer simulation of depositional sequences*. *Kansas Geological Survey, Subsurface Geology Series*, *12*, 41–42.

Enos, P., & Perkins, R. D. (1979). Evolution of Florida Bay from island stratigraphy. *Geological Society of America Bulletin*, *90*, 59–83.

Enos, P., & Samankassou, E. (1998). Lofer cyclothems revisited (Late Triassic, Northern Alps, Austria). *Facies*, *38*, 207–228.

Enos, P., & Samankassou, E. (2002). Lateral variations in Dachstein Limestone (Triassic, Austria)(abs). 16th International Sedimentological Congress (Johannesburg, South Africa), Abs. Vol., 88.

Fischer, A. G. (1964). The Lofer cyclothems of the Alpine Triassic. In D. F. Merriam (Ed.), *Symposium on cyclic sedimentation*. *Kansas Geological Survey Bulletin*, *169*, 107–149.

Forkner, R. M., Hinnov, L. A., Goldhammer, R. K., & Hardie, L. A. (2009). The allocyclic interpretation of the "Latemar Cycles" (Middle Triassic, the Dolomites, Italy) and implications for high-frequency cyclostratigraphic forcing. *Special Publication of the International Association of Sedimentologists*, *41*, 215–238.

Ginsburg, R. N. (1971). Landward movement of carbonate mud: New model for regressive cycles in carbonates (abs.). *American Association of Petroleum Geologists Bulletin*, *55*, 350.

Goldhammer, R. K., Dunn, P. A., & Hardie, L. A. (1987). High frequency glacio-eustatic sea-level oscillations with Milankovitch characteristics recorded in Middle Triassic platform carbonates in northern Italy. *American Journal of Science*, *287*, 853–892.

Goldhammer, R. K., Dunn, P. A., & Hardie, L. A. (1990). Depositional cycles, composite sea-level changes, cycle stacking patterns, and the hierarchy of stratigraphic forcing: Examples from Alpine Triassic platform carbonates. *Geological Society of America Bulletin*, *102*, 535–562.

Goldhammer, R. K., Lehmann, P. J., & Dunn, P. A. (1993). The origin of high-frequency platform carbonate cycles and third-order sequences (Lower Ordovician El Paso Group, West Texas): Constraints from outcrop data and stratigraphic modeling. *Journal of Sedimentary Petrology*, *63*, 318–359.

Goodwin, P. W., & Anderson, E. J. (1985). Punctuated aggradational cycles: A general hypothesis of episodic stratigraphic accumulation. *Journal of Geology*, *93*, 515–533.

Grotzinger, J. P. (1986). Cyclicity and paleoenvironmental dynamics, Rocknest platform, northwest Canada. *Geological Society of America Bulletin*, *97*, 1208–1231.

Haas, J. (1982). Facies analysis of the cyclic Dachstein Limestone Formation (Upper Triassic) in the Bakony Mountains, Hungary. *Facies*, *6*, 75–84.

Haas, J. (1991) A basic model for Lofer cycles. In G. Einsele, W. Ricken, & A. Seilacher (Eds.), *Cycles and events in stratigraphy* (pp. 722–732). New York, NY: Springer.

Haas, J. (1994). Lofer cycles of the Upper Triassic Dachstein platform in the Transdanubian Mid-Mountains, Hungary. In P. L. deBoer, & D. G. Smith (Eds.), *Orbital Forcing and Cyclic Sequences*, *Special Publication of the International Association of Sedimentologists*, *19*, 303–322.

Haas, J. (2004). Characteristics of peritidal facies and evidences for subaerial exposures in Dachstein-type cyclic platform carbonates in the Transdanubian Range, Hungary. *Facies*, *50*, 263–286.

Haas, J., Lobitzer, H., & Monostori, M. (2007). Characteristics of the Lofer cyclicity in the type locality of the Dachstein Limestone (Dachstein Plateau, Austria). *Facies*, *53*, 113–126.

Hardie, L. A., & Shinn, E. A. (1986). Carbonate depositional environments, modern and ancient. Part 3 – tidal flats. *Colorado School of Mines Quarterly*, *81*, 1–74.

Harris, P. M., Purkis, S. J., & Ellis, J. (2011). Analyzing spatial patterns in modern carbonate sand bodies from Great Bahama Bank. *Journal of Sedimentary Research*, *81*, 185–206.

Hill, J., Wood, R., Curtis, A., & Tetzlaff, D. M. (2012). Preservation of forcing signals in shallow water carbonate sediments. *Sedimentary Geology*, *275–276*, 79–92.

Hinnov, L. A. (2006). Discussion of "Magnetostratigraphic confirmation of a much faster tempo for sea-level change for the Middle Triassic Latemar platform carbonates" by D. V. Kent, G. Muttoni, & P. Brack. *Earth and Planetary Science Letters*, *243*, 868–873.

Husinec, A., Baschb, D., Rose, B., & Read, J. F. (2008). FISCHERPLOTS: An excel spreadsheet for computing Fischer plots of accommodation change in cyclic carbonate successions in both the time and depth domains. *Computers & Geosciences*, *34*, 269–277.

Kent, D. V., Muttoni, G., & Brack, P. (2004). Magnetostratigraphic confirmation of a much faster tempo for sea-level change for the Middle Triassic Latemar platform carbonates. *Earth and Planetary Science Letters*, *228*, 369–377.

Koerschner, W. F. III, & Read, J. F. (1989). Field and modeling studies of Cambrian carbonate cycles, Virginia Appalachians. *Journal of Sedimentary Petrology*, *59*, 654–687.

Krystyn, L., Mandl, G. W., & Schauer, M. (1991). Growth and termination of the Upper Triassic platform margin of the Dachstein area (Northern Calcareous Alps). *Austrian Journal of Earth Sciences*, *102*, 23–33.

Laporte, L. F. (1967). Carbonate deposition near mean sea-level and resultant facies mosaic: Manlius Formation (Lower Devonian) of New York State. *American Association of Petroleum Geologists Bulletin*, *51*, 73–101.

Le Blévec, T., Dubrule, O., John, C. M., & Hampson, G. J. (2018). Geostatistical modelling of cyclic and rhythmic facies architectures. *Mathematical Geosciences*, *50*, 609–637.

Lehrmann, D. J., & Goldhammer, R. K. (1999). Secular variation in parasequence and facies stacking patterns of platform carbonates: A guide to application of stacking-patterns analysis in strata of diverse ages and settings. In P. M. Harris, A. H. Saller, & J. A. Simo (Eds.), *Advances in carbonate sequence stratigraphy: Application to reservoirs, outcrops, and models*. *Society of Economic Paleontologists and Mineralogists Special Publication*, *63*, 187–225.

Milankovitch, M. (1941). *Kanon der Erdbestrahlungen und seine Anwendung auf das Eiszeitenproblem*. Belgrade: Koniglich Serbische Akademie, 633 pp.

Mundil, R., Zühlke, R., Bechstädt, T., Peterhänsel, A., Egenhoff, S. O., Oberli, F. … Rieber, H. (2003). Cyclicities in Triassic platform carbonates: Synchronizing radio-isotopic and orbital clocks. *Terra Nova*, *15*(2), 81–87.

Obermaier, M., Ritzmann, N., & Aigner, T. (2015). Multi-level stratigraphic heterogeneities in a Triassic shoal grainstone, Oman Mountains, Sultanate of Oman: Layer-cake or shingles? *GeoArabia*, *20*(2), 115–142.

Osleger, D. A. (1991a). Subtidal carbonate cycles: Implications for allocyclic vs. autocyclic controls. *Geology*, *19*, 917–920.

Osleger, D. A. (1991b). Cyclostratigraphy of Late Cambrian carbonate sequences: An interbasinal comparison of the Cordilleran and Appalachian passive margins. In J. D. Cooper, & C. H. Stevens (Eds.), *Paleozoic paleogeography of the Western United States II. Pacific section*. *Society of Economic Paleontologists and Mineralogists Field Trip Guidebook*, *67*, 811–828, Los Angeles, CA.

Osleger, D. A., & Read, J. F. (1991). Relation of eustasy to stacking patterns of meter-scale carbonate cycles, Late Cambrian, U.S.A. *Journal of Sedimentary Petrology*, *61*, 1225–1252.

Peper, T., & Cloetingh, S. (1995). Autocyclic perturbation of orbitally forced signals in the sedimentary record. *Geology*, *23*, 937–940.

Piller, W. E. (1976). Fazies und Lithostratigraphie des gebankten Dachsteinkalkes (Obertrias) am nordrand des Toten Gebirges (S Grünau/Almtal, Oberösterreich). *Mitteilungen der Gesellschaft für Geologie und Bergbaustudenten in Österreich*, *23*, 113–152.

Piller, W. E. (1981). The Steinplatte reef complex, part of an Upper Triassic carbonate platform near Salzburg, Austria. In D. F. Toomey (Ed.), *European fossil reef models*. *Society of Economic Paleontologists and Mineralogists, Special Publication*, *30*, 261–290.

Pratt, B. R., & James, N. P. (1986). The St. George Group (Lower Ordovician) of western Newfoundland: Tidal flat island model for carbonate sedimentation in shallow epeiric seas. *Sedimentology*, *33*, 313–343.

Preto, N., Hinnov, L. A., De Zanche, V., Mietto, P. and Hardie, L. A. (2004). The Milankovitch interpretation of the Latemar platform cycles (Dolomites, Italy): Implications for geochronology, biostratigraphy, and Middle Triassic carbonate accumulation. In B. D'Argenio, A. G. Fischer, I. Premoli Silva, H. Weissert & V. Ferreri (Eds.), *Cyclostratigraphy: Approaches and case histories*. *Society of Economic Paleontologists and Mineralogists Special Publication*, *81*, 167–185.

Purkis, S. J., & Harris, P. M. (2016). The extent and patterns of sediment filling of accommodation space on Great Bahama Bank. *Journal of Sedimentary Research*, *86*, 294–310.

Rankey, E. C. (2002). Spatial patterns of sediment accumulation on a Holocene carbonate tidal flat, northwest Andros Island, Bahamas. *Journal of Sedimentary Research*, *72*, 591–601.

Read, J. F. (1995). Overview of carbonate platform sequences, cycle stratigraphy and reservoirs in greenhouse and ice-house worlds. In J. F. Read, C. Kerans, L. J. Webber, J. F. Sarg, & F. M. Wright (Eds.), *Milankovitch sea-level changes, cycles, and reservoirs on carbonate platforms in greenhouse and ice-house worlds*. *Society of Economic Paleontologists and Mineralogists Short Course*, *35*, 183 pp.

Read, J. F., & Goldhammer, R. K. (1988). Use of Fischer plots to define third-order sea-level curves in Ordovician peritidal cyclic carbonates, Appalachians. *Geology*, *16*, 895–899.

Sadler, P. M., Osleger, D. A., & Montañez, P. (1993). On the labeling, length, and objective basis of Fischer plots. *Journal of Sedimentary Research*, *63*, 360–368.

Samankassou, E., Strasser, A., Di Gioia, E., Rauber, G. and Dupraz, C. (2003). High-resolution record of lateral variations on a shallow carbonate platform (Upper Oxfordian, Swiss Jura Mountains). *Eclogae Geologicae Helvetiae*, *96*, 425–440.

Sander, B. (1936) Beiträge zur Kenntnis der Ablagerungsgefhge (rhythmische Kalke und Dolomite aus der Trias). *Tschermaks Mineralogische Und Petrographische Mitteilungen*, *48*, 27–209.

Satterley, A. K. (1996a) The interpretation of cyclic successions of the Middle and Upper Triassic of the Northern and Southern Alps. *Earth-Science Reviews.*, *40*(3–4), 181–207.

Satterley, A. K. (1996b) Cyclic carbonate sedimentation in the Upper Triassic Dachstein Limestone, Austria: The role of patterns of sediment supply and tectonics in a platform-reef-basin system. *Journal of Sedimentary Research*, *66B*, 307–323.

Schwarzacher, W. (1948). Über sedimentäre Rhythmik des Dachsteinkalkes am Lofer. *Geologisches Bundesanstalt, Wien, Verhandlung, Heft*, *10–12*, 176–188.

Schwarzacher, W. (1954). Die Grossrhythmik des Dachstein Kalkes von Lofer. *Tschermaks Mineralogische und Petrographische Mitteilungen*, *4*, 44–54.

Schwarzacher, W. (2005). The stratification and cyclicity of the Dachstein Limestone in Lofer, Leogang and Steinernes Meer (Northern Calcareous Alps, Austria). *Sedimentary Geology*, *181*, 93–106.

Spahn, Z. P., Kodama, K. P., & Preto, N. (2013). High-resolution estimate for the depositional duration of the Triassic Latemar Platform: A new magnetostratigraphy and magnetic susceptibility cyclostratigraphy from basinal sediments at Rio Sacuz, Italy. *Geochemistry, Geophysics, Geosystems*, *14*, 1245–1257.

Spencer, R. J., & Demicco, R. V. (1989). Computer models of carbonate platform cycles driven by subsidence and eustasy. *Geology*, *17*, 165–168.

Tipper, J. C. (1998). The influence of field sampling area on estimates of stratigraphic completeness. *Journal of Geology*, *106*, 727–739.

Wanless, H. R. (1979). Role of physical sedimentation in carbonate bank growth (abs.). *American Association of Petroleum Geologists Bulletin*, *63*, 547.

Wanless, H. R. (1981). Fining- upward sedimentary sequences generated in seagrass beds. *Journal of Sedimentary Petrology*, *51*(2), 445–454.

Wilkinson, B. H., & Drummond, C. N. (2004). Facies mosaics across the Persian Gulf and around Antigua – Stochastic and deterministic products of shallow-water sediment accumulation. *Journal of Sedimentary Research*, *74*, 513–526.

Wilkinson, B. H., Drummond, C. N., Diedrich, N. W., & Rothman, E. D. (1997). Biological mediation of stochastic peritidal carbonate accumulation. *Geology*, *25*, 847–850.

Wright, V. P. (1992). Speculations on controls on peritidal carbonates: Ice-house versus greenhouse eustatic controls. *Sedimentary Geology*, *76*, 1–5.

Yang, W., Mazzullo, S. J., & Teal, C. S. (2004). Sediments, facies tracts, and variations in sedimentation rates of Holocene platform carbonate sediments and associated deposits, northern Belize – Implications for "representative" sedimentation rates. *Journal of Sedimentary Research*, *74*, 498–512.

Zankl, H. (1967). Die Karbonatsedimente der Obertrias in den Nördlichen Kalkalpen. *Geologische Rundschau*, *56*, 128–139.

Zühlke, R. (2004).Integrated cyclostratigraphy of a model Mesozoic carbonate platform—The Latemar (Middle Triassic, Italy). In B. D'Argenio, A. G. Fischer, I. Premoli-Silva, H. Weissert, & V. Ferreri (Eds.), *Cyclostratigraphy: Approaches and case histories*. *Society of Economic Paleontologists and Mineralogists Special Publication*, *81*, 183–211.

Zühlke, R., Bechstadt, T., & Mundil, R. (2003). Sub-Milankovitch and Milankovitch forcing on a model Mesozoic carbonate platform – The Latemar (Middle Triassic, Italy). *Terra Nova*, *15*, 69–80.

How to cite this article: Samankassou E, Enos P. Lateral facies variations in the Triassic Dachstein platform: A challenge for cyclostratigraphy. *Depositional Rec*. 2019;5:469–485. https://doi.org/10.1002/dep2.80